Lithuanian Journal of Physics, Vol. **46**, No. 1, pp. 67–72 (2006) doi:10.3952/lithjphys.46107

INVESTIGATION OF STRUCTURE AND CARRIER RECOMBINATION IN $TlGaSe_2$ LAYERED CRYSTALS

V. Grivickas [a], V. Bikbajevas [a], M.I. Tarasik [b], and A.K. Fedotov [b]

[a] *Institute of Materials Science and Applied Research, Vilnius University, Saulėtekio 10, LT-10223 Vilnius, Lithuania*
E-mail: vytautas.grivickas@ff.vu.lt

[b] *Department of Energy Physics, Belarusian State University, F. Skaryna Ave. 4, 220050 Minsk, Belarus*

Received 8 November 2005

Large size $TlGaSe_2$ layered crystals grown by Bridgman method have been investigated by x-ray microanalysis and scanning electron microscopy. The mechanism of excess free carrier recombination after a high level laser pulse excitation performed in a high quality sample has been investigated. It has been shown that, in high injection region, the carrier lifetime is mainly determined by Auger recombination. The Auger recombination coefficient is established to be about $1{\cdot}10^{-29}$ cm^6/s. In low injection region, minority carrier trapping is observed. The longest exponential majority carrier constant lifetime is equal to 6 ms at 70 K.

Keywords: layered chalcogenides, crystal stoichiometry, carrier recombination, Auger recombination, carrier lifetime

PACS: 61.50.Nw, 72.20.Jv, 78.47.+p

1. Introduction

The ternary compound $TlGaSe_2$ crystals belong to the class of complex semiconducting chalcogenides ABX_2 (where X is chalcogen S, Se, Te). They are layer and chain crystals that can be represented by monoclinic structure of 32 atoms in the elementary cell and the $C_{2/c}$ (C^6_{2h}) space group [1]. Stacking of atoms in the crystal is arranged in a form of two twisted anionic layers with a weakly bonded Tl^+ cations located in the trigonal cavities between them. Therefore, crystals consist of separate layers with strong bonding between atoms within a layer and weak bonding between the layers. Recently, such semiconductor crystals received a great deal of attention due to their optical and electrical properties in view of possible optoelectronic device application [2]. In this case it is necessary to clarify the processes of recombination and to determine the lifetime of minority carriers in the material. Up to now, very few investigations have been performed on the subject in earlier photoconductivity studies under low injection levels [3–5]. To the best of our knowledge, analogous research in the range of high excitation has not been carried out. So, the main objective of this study is to investigate the recombination processes and to determine the carrier lifetime mechanisms in $TlGaSe_2$ at high excitation level.

2. Structural investigation

Samples used for investigation were synthesized from the high purity elements taken in stoichiometric proportions. Large size platelets of a few millimetre thicknesses and of several square centimetres were grown by Bridgman method [6]. Crystals showed weak p-type conduction at room temperature. Some platelets contain a number of flaky-damaged plains. These particular platelets have weaker mechanical rigidity in term of slicing, while some other ones were characterized by much higher rigidity and optical uniformity. For those platelets, in their band edge absorption spectrum taken at low (15 K) temperature, direct exciton peaks and indirect excitonic steps have been clearly identified [7].

In order to distinguish the samples, we have performed their scanning electron microscopy and x-ray microanalysis using LEO1455VP apparatus (*Karl Zeiss*) equipped with SiLi detector (*Rontec*). A few electron scan images at 20 keV electron energy obtained for mechanically defective sample surface are shown in Fig. 1. A number of separated inclusions (particles) or fragments of different shape and size, can be distinguished on the surface. Most of them are stuck in the terrace boundary regions (Fig. 1(a, b)). Qualitative measurement of element composition, as shown in Fig. 2, was performed along certain sample surface lines. It shows that some inclusions clearly have en-

ISSN 1648-8504

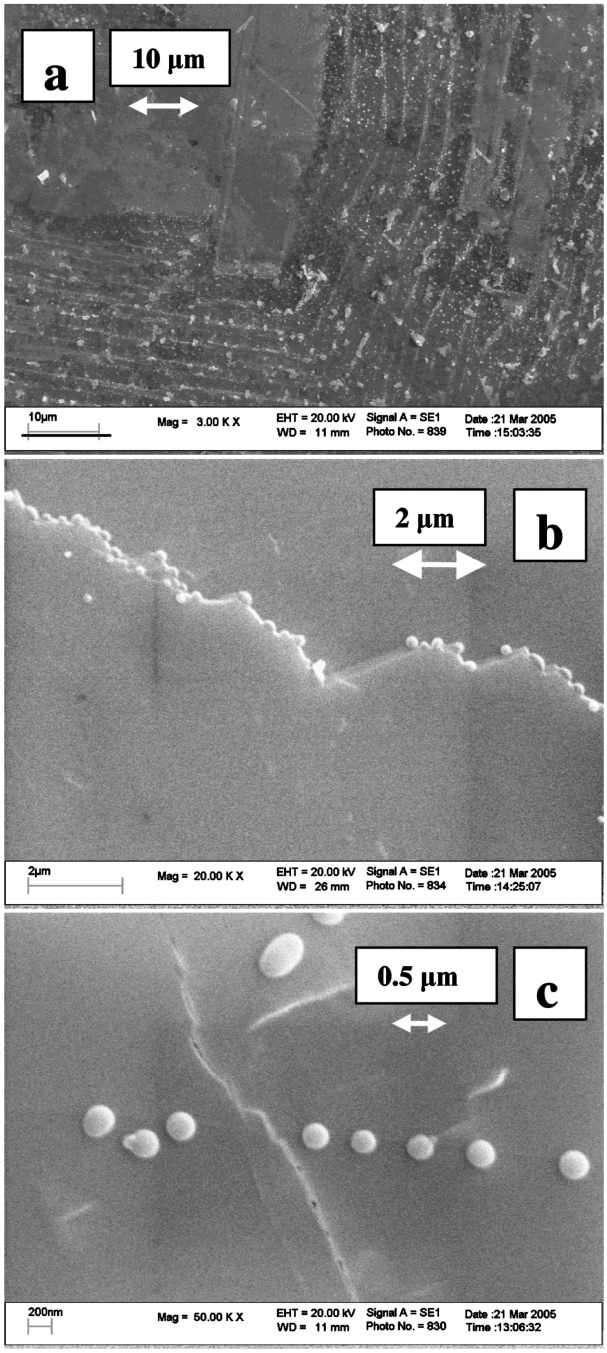

Fig. 1. Scanning electron microscopy images of the defective $TlGaSe_2$ surface areas with different resolution: (a) 10 μm, (b) 2 μm, (c) 0.5 μm. A number of different size particles are mainly located in terrace boundary regions.

riched content of Se and reduced content of Ga. Other ones have another type of nonstoichiometric differences, for example, increase of Se and reduction of Tl while Ga is almost unchanged. On the other hand, the small particles of elliptical shape (such as in Fig. 1(c)) were defined as Tl precipitates without noticeable content of other two elements. Taking into account x-ray intensity of the characteristic energy lines and effective volume of the excitation, we have performed a mathematical data processing of absolute element ratios. Then we have found that, within the experimental error range, the composition of $TlGaSe_2$ compound in plain areas of the samples without any type of fragments and precipitates falls into the stoichiometric ratio range.

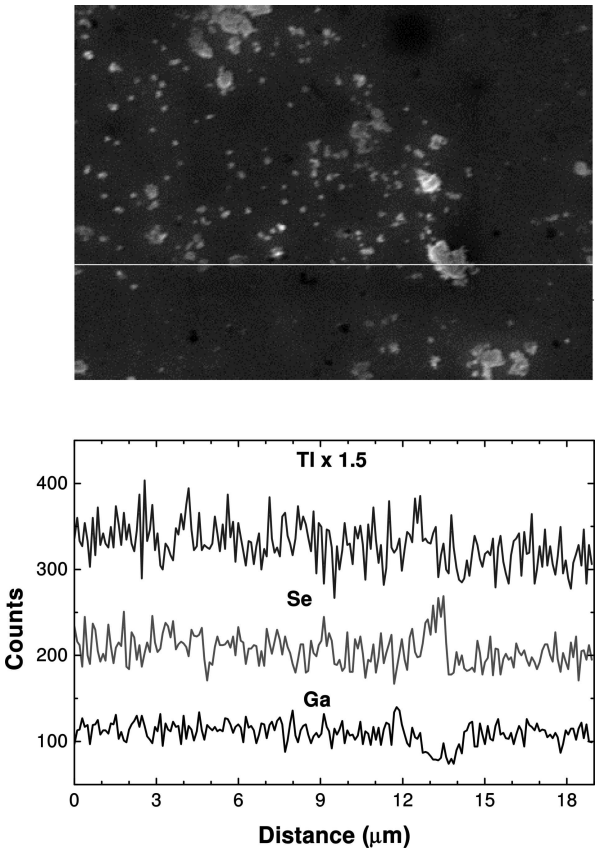

Fig. 2. Element content distribution along the line of the defective area.

These results can be interpreted as follows. During the growth, a substantial disturbance of the stoichiometry can take place in certain areas of crucible during prolonged time of cooling in the range of 950–1150 K. The excess of some elements in $TlGaSe_2$ crystal precipitates and forms the inclusions. Some of those precipitates are incorporated between layer planes and weaken mechanical properties of platelets; others are released in outer part of crucible. On the other hand, quite large areas of crystal are grown without substantial disturbances.

In Fig. 3 a lateral view of the uniform platelet with visible layer sides is shown. The overall surface is almost perpendicular to the layer (100) plane, and only small roughness associated with presence of multitude layer distortion can be observed. Such platelets were slabs of a 4×8 mm^2 size with thickness of about 2 mm. They have been carefully polished on both sides of layers cross cut planes. After polishing, damaged side

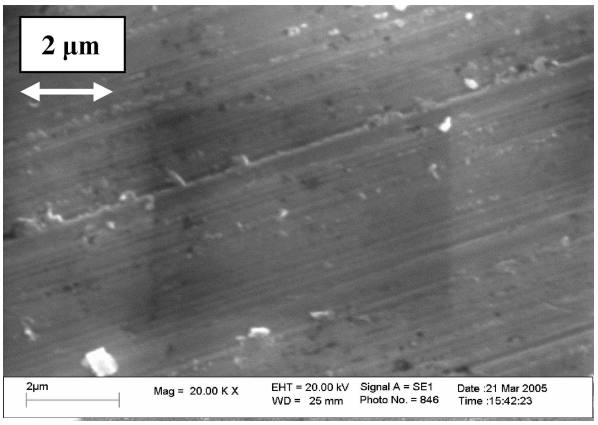

Fig. 3. Scanning electron microscopy image of lateral sample side before polishing. Layer planes are clearly visible.

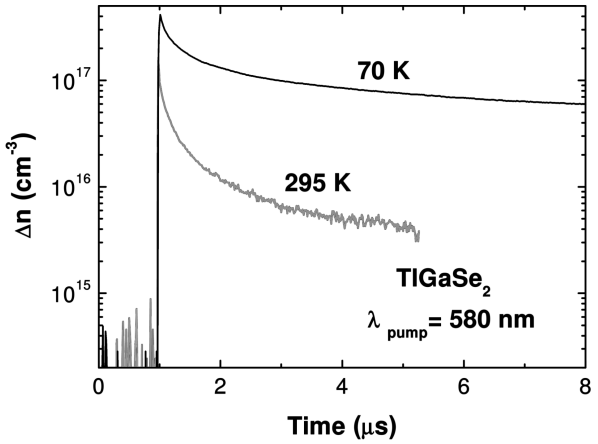

Fig. 4. An example of excess free carrier decays at 295 and 70 K.

parts of each sample were cleaved off along the basal plane, i. e. parallel to the layers. As the result, a rectangular shape and optically homogeneous samples of about $2\times6\times0.45$ mm^3 dimension have been obtained for pump-probe investigation of carrier recombination.

3. Free carrier absorption

Selected and optically polished $TlGaSe_2$ sample of high quality was placed on a cold finger of nitrogen optical cryostat. Sample was homogeneously excited with 580 nm wavelength and 2.5 ns width at half-maximum amplitude pulses from a tunable wavelength optical parametric oscillator, which was pumped by Nd:YAG laser. The pulse repetition rate was 40 Hz and the maximum laser fluence per pulse was 0.25 mJ/cm^2. Free carrier absorption signal was detected using a 1.3 μm focused infrared probe beam directed from the perpendicular side. The details of the measurement set-up can be found in Refs. [8, 9]. The photoinduced absorption transient $\Delta\alpha(t)$ was recorded in a real time mode using a digital oscilloscope with a 1 ns sampling resolution. The signals were averaged over 500 signal traces to reduce the noise level. Carrier concentration value was estimated from the relation $\Delta n = \Delta p = \Delta\alpha/\sigma_{\rm eh}$ where $\sigma_{\rm eh}$ is free electron–hole pair cross-section described in Ref. [7].

4. Lifetime results

Figure 4 shows an example of excess carrier decays at 70 and 295 K. As one can see the decays are nearly hyperbolic in the beginning part of decay. For better visualization of decay process several measurements with various initial values of injected excess carrier

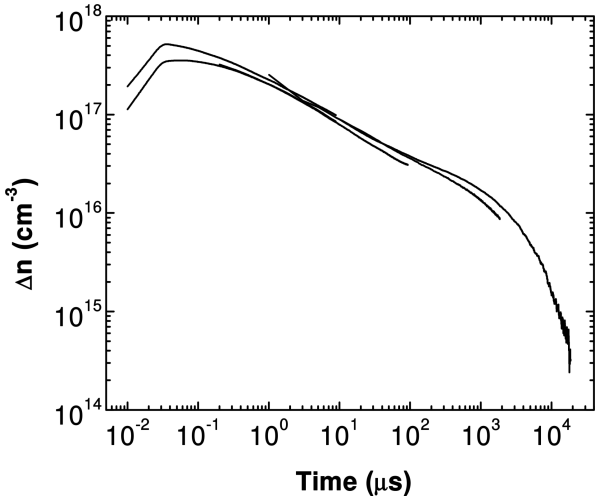

Fig. 5. Excess free carrier decays after pump laser pulses with various time resolutions to cover a wide range of the concentration change in log–log scale.

concentration and different time resolution have been performed. The result of the measurement at 70 K is shown in Fig. 5. For obviousness the obtained data are presented in a log–log scale. The derived relationship provides a way for calculation of instantaneous lifetime values as a function of carrier concentration [9]. Figure 6 presents such plot where distinct symbols identify sets of data determined from different decays in Fig. 5. As seen, the lifetime varies proportionally to Δn^{-2} when carrier concentration is more than $2{\cdot}10^{17}$ cm^{-3}. At excess carrier concentration of about $4{\cdot}10^{16}$ and $3{\cdot}10^{16}$ cm^{-3} a reduction and then increase of the slope occurs. In the low injection region ($\Delta n < 10^{16}$ cm^{-3}) decay saturates at lifetime of about 6 ms.

Other measurements of the decay have been performed with different probe beam wavelength and polarizations with respect to the crystal **c**-axis. These (not shown) results can be summarized as follows. A

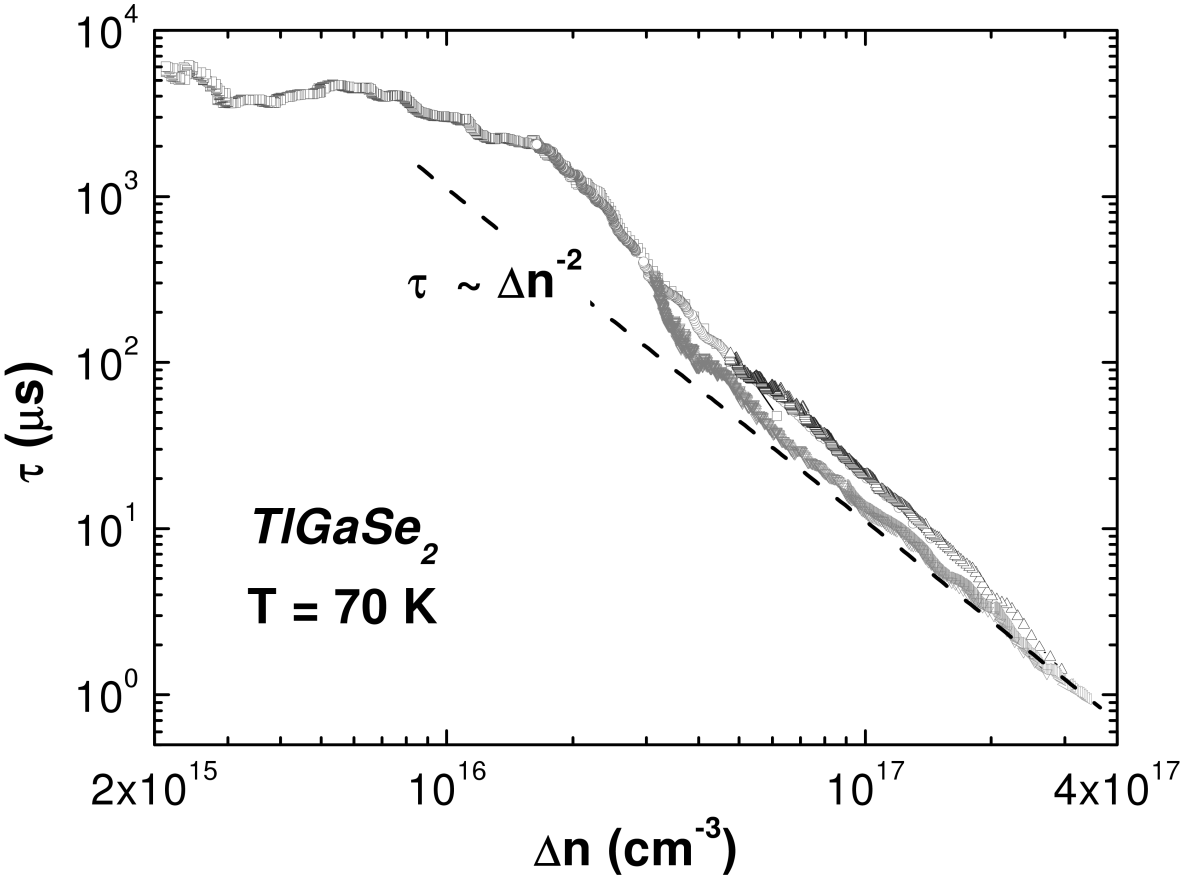

Fig. 6. Instantaneous excess free carrier lifetime versus their concentration. Each type of symbol represents result obtained from single Δn decay. The lifetimes associated with Auger recombination are shown by dashed line.

lifetime variation proportional to Δn^{-2} in high level injection region is observed in all measurements. In the intermediate injection range, τ versus Δn relationship slope takes different values depending on the probe beam wavelength and polarization. A part of decay at low injection in all cases is ending with the similar constant lifetime. The value of this lifetime increases from $10-15$ μs to $5-7$ ms when temperature decreases from 300 down to 70 K.

In the generally accepted model of injection and recombination processes in three-dimensional bulk material the equality between excess electrons and holes ($\Delta n = \Delta p$) is assumed to be valid all the time. The overall recombination lifetime τ can be expressed by the inverse sum of the inverse lifetime additives [9]:

$$\tau = \left(\tau_{\mathrm{SRH}}^{-1} + \tau_{\mathrm{S}}^{-1} + \tau_{\mathrm{r}}^{-1} + \tau_{\mathrm{tA}}^{-1} + \tau_{\mathrm{A}}^{-1}\right)^{-1}. \qquad (1)$$

Here τ_{SRH}^{-1} is impurity centre related (Schockley–Read–Hall) lifetime, τ_{S}^{-1} is surface related lifetime, τ_{r}^{-1} is radiative, τ_{tA}^{-1} is trap-assisted Auger lifetime, and τ_{A}^{-1} is band-to-band Auger recombination lifetime [8]. In $TlGaSe_2$ we may neglect surface related and radiative lifetimes because of the low diffusion to the surfaces [7] and negligible radiation probability [10], respectively. We also assume that trap-assisted Auger recombination is not important. The band-to-band Auger recombination lifetime term $\tau_{\mathrm{A}} = 1/(\gamma \Delta n^2)$ in tree-dimensional model is in close agreement with observed dependence. By applying this relationship (dashed line in Fig. 6) we obtain Auger recombination coefficient to be equal to about $1{\cdot}10^{-29}$ cm^6/s. To the best of our knowledge, the value of Auger recombination coefficient in $TlGaSe_2$ crystal is reported for the first time.

In the intermediate injection range, the observed differences of lifetime obtained using various probe beam polarizations and wavelengths can be explained in the following way. In the general case the free carrier absorption coefficient $\Delta\alpha = \sigma_{\mathrm{e}} \cdot \Delta n + \sigma_{\mathrm{h}} \cdot \Delta p$, where $\sigma_{\mathrm{e(h)}}$ is free electron (hole) absorption cross section. The value of $\Delta\alpha$ is determined by superior component. We assume that condition $\Delta n = \Delta p$ is no longer obeyed in the intermediate injection region and part of one or of both types of excess free carriers is trapped. Furthermore, for the direct intraband mechanism of free carrier absorption (i. e. vertical optical transitions without phonon contribution), the ratio $\sigma_{\mathrm{e}}/\sigma_{\mathrm{h}}$ can vary with

probe beam wavelength and its polarization depending on the symmetry of the bands. A good example of σ_e/σ_h changes (so called Biedermann bands) was observed in anisotropic hexagonal semiconductors such as SiC polytypes [11]. The same situation could be expected in our case. However, in contrast to SiC, the σ_e and σ_h dependence on the wavelength is not known for $TlGaSe_2$ since it is impossible to get highly doped crystals of such layered material. We assume that after pump laser pulse part of electrons are captured and recombination velocity of holes via deep centres determines a constant free carrier lifetime at the end of the decay process.

5. Conclusions

We have investigated the structure and carrier recombination in high quality $TlGaSe_2$ layered crystals. It was shown for the first time that the main recombination mechanism at high level injection region is the Auger recombination, as in bulk crystals. This result is consistent with a three-dimensional model applied for explanation of an excitonic absorption edge in $TlGaSe_2$ [7] and other layered semiconductors [12].

Acknowledgements

This study is supported by Swedish Visby program and by the Lithuanian State Science and Studies Foundation.

References

[1] S. Ves, Effects of hydrostatic pressure on the fundamental absorption edge of $TlGaSe_2$, Phys. Rev. B **40**(11), 7892–7897 (1989).

[2] V. Grivickas, V. Bikbajevas, and J. Linnros, Strong absorption undulations created by photoacoustic pulses in layered $TlGaSe_2$ crystals (unpublished).

[3] V.A. Aliev and G.D. Guseinov, Recombination process in nonstoichiometric $TlGaSe_2$, Sov. Phys. – Semicond. **19**(11), 1940–1943 (1985).

[4] G.D. Guseinov, V.A. Aliev, and E.F. Bagirzade, Recombination levels in non-stoichiometric $TlGaSe_2$, Phys. Status Solidi A **94**(2), 653–657 (1986).

[5] I.M. Ashraf, M.M. Abdel-Rahman, and A.M. Badr, Photoconductivity of $TlGaSe_2$ layered single crystals, J. Phys. D **36**(2), 109–113 (2003).

[6] V.A. Aliev and G.D. Guseinov, Imperfections in single crystals of $TlGaSe_2$, Inorg. Mater. (USSR) **23**(2), 301–303 (1987).

[7] V. Grivickas, V. Bikbajevas, and P. Grivickas, Indirect absorption edge of $TlGaSe_2$ crystals, Phys. Status Solidi B, **243**(5), R31–R33 (2006); V. Grivickas et al. (unpublished).

[8] V. Grivickas, A. Galeckas, P. Grivickas, J. Linnros, and V. Bikbajevas, Excess free carrier optical excitation spectroscopy in indirect semiconductors, Mater. Sci. (Medžiagotyra) **7**(4), 203–208 (2001).

[9] J. Linnros and V. Grivickas, in: *Methods in Materials Research*, ed. E.N. Kaufmann (John Wiley & Sons, New York, 2000) pp. 5b.2.1–31.

[10] N.M. Gasanly, A. Serpenguzel, A. Aydinli, and S.M.A. Baten, Low-temperature visible photoluminescence spectra of $TlGaSe_2$ layered crystal, J. Lumin. **86**(1), 39–43 (2000).

[11] V. Grivickas, A. Galeckas, P. Grivickas, and J. Linnros, Determination of the polarization dependence of the free-carrier-absorption in 4H-SiC at high-level photoinjection, Mater. Sci. Forum **338–342**, 555–558 (2000).

[12] J. Camassel, P. Merle, H. Mathieu, and A. Chevy, Excitonic absorption edge of indium selenide, Phys. Rev. B **17**(12), 4718–4724 (1978).

STRUKTŪRINIAI BEI KRŪVININKŲ REKOMBINACIJOS TYRIMAI $TlGaSe_2$ SLUOKSNIUOTUOSE KRISTALUOSE

V. Grivickas [a], V. Bikbajevas [a], M.I. Tarasik [b], A.K. Fedotov [b]

[a] *Vilniaus universieto Medžiagotyros ir taikomųjų mokslų institutas, Vilnius, Lietuva*
[b] *Baltarusijos valstybinis universitetas, Minskas, Baltarusija*

Santrauka

Didelių matmenų $TlGaSe_2$ kristalai, išauginti Bridžmano būdu, buvo tiriami skenuojančiu mikroskopu ir analizuojami antrinių rentgeno spindulių spektroskopijos metodu. Perteklinių krūvininkų rekombinacija buvo tiriama žadinant lazerio impulsu, matuojant laisvakrūvę sugerties relaksaciją. Parodyta, kad didelės injekcijos atveju krūvininkų gyvavimo trukmę lemia Ožė rekombinacijos mechanizmas. Gautas Ožė rekombinacijos koeficiento dydis yra apie 10^{-29} cm^6/s. Mažesnės injekcijos srityje stebimas nepagrindinių krūvininkų prilipimas. Ilgiausia pagrindinių krūvininkų eksponentinės relaksacijos trukmė siekia 6 ms, kai $T = 70$ K.